

CONF-8810402--1

MICROSTRUCTURAL AND MINERALOGICAL CHARACTERIZATION OF SELECTED
SHALES IN SUPPORT OF NUCLEAR WASTE REPOSITORY STUDIES

CONF-8810402--1

DE89 015906

S. Y. Lee, L. K. Hyder, and P. D. Alley

Environmental Sciences Division

Oak Ridge National Laboratory

P. O. Box 2008

Oak Ridge, TN 37831-6317

DISCLAIMER

This report was prepared as an account of work sponsored by an agency of the United States Government. Neither the United States Government nor any agency thereof, nor any of their employees, makes any warranty, express or implied, or assumes any legal liability or responsibility for the accuracy, completeness, or usefulness of any information, apparatus, product, or process disclosed, or represents that its use would not infringe privately owned rights. Reference herein to any specific commercial product, process, or service by trade name, trademark, manufacturer, or otherwise does not necessarily constitute or imply its endorsement, recommendation, or favoring by the United States Government or any agency thereof. The views and opinions of authors expressed herein do not necessarily state or reflect those of the United States Government or any agency thereof.

To be published in

CLAY MICROSTRUCTURE-FROM MUDS TO SHALE

in series

FRONTIERS IN SEDIMENTARY GEOLOGY

DISTRIBUTION OF THIS DOCUMENT IS UNLIMITED

MICROSTRUCTURAL AND MINERALOGICAL CHARACTERIZATION OF SELECTED
SHALES IN SUPPORT OF NUCLEAR WASTE REPOSITORY STUDIES¹

S. Y. Lee, L. K. Hyder, and P. D. Alley²

Environmental Sciences Division

Oak Ridge National Laboratory

ABSTRACT

Five shales were examined as part of the Sedimentary Rock Program evaluation of this medium as a potential host for a U.S. civilian nuclear waste repository. The units selected for characterization were the Chattanooga Shale from Fentress County, Tennessee; the Pierre Shale from Gregory County, South Dakota; the Green River Formation from Garfield County, Colorado; and the Nolichucky Shale and Pumpkin Valley Shale from Roane County, Tennessee.

The micromorphology and structure of the shales were examined by petrographic, scanning electron, and high-resolution transmission electron microscopy. Chemical and mineralogical compositions were studied through the use of energy-dispersive X ray, neutron activation, atomic absorption, thermal, and X-ray diffraction analysis techniques.

¹Research sponsored by the Geoscience Technology Support Program, U.S. Department of Energy, under contract DE-AC05-84OR21400 with Martin Marietta Energy Systems, Inc. Publication No. 0000, Environmental Sciences Division, Oak Ridge National Laboratory.

²Miami University, Oxford, Ohio.

The Chattanooga Shale was highly compacted and its micropores filled with organic materials, and spores, compressed along bedding planes, were common. Very thin beds, rich in silt-size quartz grains, alternated with a clay- and organic-rich matrix so as to create discontinuous laminae. Illite, quartz, and organic matter were major components in the shale. In the Pierre Shale, there was slight preferential particle orientation. Microfractures were common and frequently filled with carbonate and sulfide minerals. Montmorillonite, calcite, and quartz were the dominant minerals. The Green River Formation sample was hard and extensively cemented with amorphous silica and carbonate. Such cementation gave physical stability to the shale and locked kerogen in isolated micropores. Dolomite, quartz, kerogen, and illite were dominant components in the sample. The Nolichucky Shale had a high degree of preferential particle orientation. It was composed of illite, quartz, feldspar, chlorite, kaolinite, and carbonate minerals. A major portion of the carbonate was fracture-filling secondary calcite, but detrital dolomite and calcite were also observed. The Pumpkin Valley Shale, a laminated mudstone and siltstone, had illite, quartz, feldspar, chlorite, and kaolinite minerals. Clay particles in the shale were loosely packed and randomly oriented. Carbonate cementation was rarely observed in the mudstone but was common in the siltstone laminae.

The morphological and mineralogical characteristics of the shales have an important role in the determination of their suitability as possible hosts for a nuclear waste repository because these characteristics directly relate to geochemical, geophysical, and geohydrological performance of the rock formations.

INTRODUCTION

The Sedimentary Rock Program at Oak Ridge National Laboratory (ORNL) has evaluated a variety of sedimentary rocks as potential host media for a U.S. civilian nuclear waste repository. Shale was selected as the sedimentary rock with the greatest potential, based on technical aspects related to geology, geochemistry, hydrology, thermal performance, rock mechanics, natural resources, waste package material degradation, repository costs, and systems studies (Croff et al. 1986). Other countries such as Belgium, Italy, Switzerland, and the United Kingdom are considering argillaceous formations as a potential host rock for high-level waste disposal (Gera 1980).

Because shales are a diverse and highly variable type of rock, complete characterization of all types would be a formidable task. Therefore, four end-members that represent the spectrum of shales were identified based on differences in their chemical and mineralogical compositions (Stow and Croff 1987). The end-members selected for characterization are organic-, carbonate-, smectite-, and illite-rich shales. The microstructure and mineralogy not only influence radionuclide migration but also influence the hydrologic and mechanical properties of the host rock (Lee and Tank 1985, Güven et al. 1988, Milodowski et al. 1985, Von Damm 1987, Weaver 1979, Burkett et al. 1987, and Lomenick and Laughon 1980). Therefore, microstructure and mineralogical data should be acquired and compiled as a basis for further investigations. The objective of this study was to conduct the microstructure and mineralogical

characterization of the end-member shales in support of nuclear waste repository studies.

MATERIALS AND METHODS

Materials

Five core samples, representing the four end-member shale compositions, were selected for microstructure and mineralogical characterization studies. The shales selected were Chattanooga Shale (organic), Pierre Shale (smectitic), Green River Formation (carbonate), and Nolichucky Shale and Pumpkin Valley Shale (illitic). The Pierre Shale and Green River Formation core samples were obtained from RE/SPEC, Inc. (Rapid City, South Dakota), and samples of the other shales were collected by ORNL geologists.

The Chattanooga Shale sample was from the upper Dowelltown Member of the formation in Fentress County, Tennessee, at a depth of 141 to 142 m. This unit is generally described as interbedded, medium light grey claystone and dark grey shale beds, 3 to 12 cm thick (Conant and Swanson 1961).

The Pierre Shale samples (PS/86/20U13-1T/2 and PS/86/20U13) were from the Mobridge Member of the Pierre Shale in Gregory County, South Dakota. They were retrieved from drill hole 84-20 at a depth of 88.2 to 88.9 m. The samples were described as claystone, thick bedded to massive, nonfissile, slightly to moderately calcareous, soft, moist, medium gray with a slight olive tinge, dense, solid, bedding at low angle, and nonweathered.

The Green River Formation samples (GR/86/V33-0/2-3/1 and GR/86/V22-0) were from Garfield County, Colorado. They were obtained from the roof of the Colony Mine from two separate but closely adjacent drill holes

(about 1.8 and 0.9 m from the back of the mine). The samples were described as thinly bedded calcareous marl, very hard and compact.

The Nolichucky Shale and Pumpkin Valley Shale were from the Joy 2 well in Oak Ridge, Tennessee, at depths of 181 to 182 m and 604 to 605 m, respectively. Both shales belong to the Conasauga Group, a complex sequence of Middle to Upper Cambrian clastic and carbonate strata that outcrops throughout the Valley and Ridge Province. The Nolichucky section is described from the well log as a grey to brown shaly siltstone with discontinuous parallel bedding. The Pumpkin Valley section is a maroon-to-grey, glauconitic, laminated, silty mudstone.

Methods

Each core segment was vertically split into two half cores, and one of the half cores was broken with a rock hammer into small fragments (<3 cm). The fragments were crushed manually with mortar and pestle until they passed through a 2-mm-mesh sieve, and then they were pulverized for 10 to 15 min in a Siebtechnik mechanical "shatterbox" consisting of an agate liner, ring, and disk. The resultant rock powder was sieved through 0.18-mm mesh. Any material that did not pass through the sieve was repulverized by hand with an agate mortar and pestle and resieved. The remaining half of each core segment was used to make specimens for microstructure analyses.

The micromorphology and structure of the shales were examined by petrographic microscopy and scanning electron microscopy (JEOL JSM-840A). Semiquantitative chemical compositions of the surface and the polished cross-section surfaces of the shales were determined by a Tracor Northern

energy-dispersive X-ray analyzer (EDX) attached to the scanning electron microscope. For high-resolution transmission electron microscopy, thin sections of the samples were cut perpendicular to the bedding plane to promote optimum orientation for lattice-fringe imaging of phyllosilicates. Following optical examination, selected areas (3 mm in diameter) were detached, ion-thinned on a cold stage, and carbon coated. The ion-thinned samples were examined at 200 kV in a JEOL JEM-2000FX transmission electron microscope with attached Tracor Northern EDX system. One-dimensional lattice-fringe images were obtained by using (001) diffractions (Lee et al. 1975a).

Multielement neutron activation analyses of the pulverized shales were performed with the ORNL Research Reactor (Lee et al. 1987). After acid dissolution of the samples, selected elements were analyzed by atomic absorption by the ORNL Analytical Chemistry Division. Total sulfur and sulfide were determined with an automatic LECO titrator. The amount of inorganic carbonate in the shales was determined by measuring the volume of CO_2 that evolved from the reaction of carbonates with excess HCl (Lee et al. 1987). Surface area was determined by measuring the amount of nitrogen adsorbed at liquid nitrogen temperature (standard BET method) on the surface of shale samples. Thermal gravimetric analyses and differential thermal analyses were performed on the samples over a temperature range of 30 to 1100°C with a Netzsch STA-429 thermobalance (data were shown in Lee et al. 1987).

Ten grams of pulverized shales (<180- μm grain size) was treated with 100 mL of 1 N sodium acetate in a warm water bath for 24 h to disperse the carbonates for geochemical fractionation. The shale residue was digested

by the addition of 30% hydrogen peroxide while being heated in a warm water bath until the reaction ceased (to remove organics). The supernates from this and the previous treatment were collected for later analysis. Iron minerals and coatings were removed by washing the shale residue with sodium acetate, then treating it with dithionite in three 1-g increments while stirring in 50 mL of 1 M sodium bicarbonate and 0.3 M citrate solution (Jackson 1975). The supernate from this treatment was held for analysis, and the residue was filtered through a 53- μm sieve. A 9-cm column of the <53- μm fraction was suspended in a dilute sodium carbonate solution, centrifuged at 750 rpm for 2.9 min, and the <2- μm fraction of supernate decanted. Similarly the <2- μm fraction was centrifuged at 2400 rpm for 31.4 min to separate the <0.2- μm fraction. The <0.2- μm fraction was divided into two aliquots for X-ray diffraction analysis; one was treated with 0.1 N potassium chloride, the other with 0.1 N magnesium chloride.

X-ray diffraction (XRD) analyses were performed on samples of the various heavy liquid and grain-size fractions with a Phillip's powder X-ray diffractometer. Samples were prepared for analysis by transferring potassium- or magnesium-saturated ethanol slurries of the sediments to glass slides, air drying them, then bombarding them with copper $\text{K}\alpha$ radiation. The potassium-saturated samples were heated to 550°C after XRD and the magnesium-saturated samples were glycolated before being run in the diffractometer to aid in identification.

RESULTS AND DISCUSSION

Petrographic Microscopy

Thin sections of the selected shale samples were examined to observe mineral constituents in their natural, undisturbed arrangement. Since shales consist almost exclusively of clay minerals and very fine particles, it was extremely difficult to identify all of their components petrographically.

The Chattanooga Shale was relatively uniform in texture and composition (Fig. 1A). The color in transmitted light was predominantly dark brown to black, representing mostly amorphous organic matter (kerogen). Compressed spores, frequently filled with frambooids and individual crystals of pyrite, were common. Very thin beds, rich in silt-size (20- to 40- μm) detrital quartz grains alternated with a clay- and organic-rich matrix so as to create discontinuous laminae, 10 to 30 μm thick. Occasionally, a microfracture filled with calcite, secondary quartz, and/or pyrite was observed. Clay minerals were mixed uniformly with organic matter throughout the area examined, except for a burrow that was filled with randomly oriented clay and detrital minerals.

The Pierre Shale consisted of mottled brown, black, and yellow areas, with translucent grains in transmitted light (Fig. 1B). The black areas were concentrations of amorphous organic material and varying sizes (10 to 50 μm) of pyrite crystals. The brown, black, and yellow areas were a mixture of clays (40 to 50%) and detrital grains. The translucent grains were quartz and calcite. Blocky calcite filled thin fractures and pores. Silt-size quartz particles were uniformly distributed. Gastropod and

ostracod shells were present and associated with pyrite and amorphous kerogen. The shells were often filled with blocky calcite. The shale had a uniform texture with no apparent lamination, but the mineral grains displayed a preferred orientation.

The Green River Formation was extremely fine grained (<10 μm) and composed mainly of dolomite, quartz, kerogen, and feldspars. The sample was uniform in texture but could be divided into two areas based on color in transmitted light. The first region was distinctly laminated (Fig. 1C). The laminations were 20 to 150 μm thick; ranged from red to orange, brown, and yellow; and were continuous, cross bedded, and disrupted only by soft-sediment deformation. Quartz grains were uniformly distributed. The second region was uniform in grain size (about 10 μm), yellow in color, and devoid of observable lamination. Detrital quartz grains were evenly distributed throughout the area. Heavy minerals were uniformly distributed in both zones, but occasionally a higher concentration was found at the interface between laminated and homogeneous regions (Fig. 1D).

The Nolichucky Shale consisted of yellow to brown clay with stringers of black amorphous organic matter and scattered translucent Ca^{+} grains. The detrital grains of calcite, quartz, and feldspars were 10 μm or less in size. Clays were most abundant and preferentially oriented along bedding planes. Thin (<10- μm) and short (50- to 300- μm) stringers, apparently filled with organic material, were observed. Stair-step fractures were another prominent feature of the Nolichucky Shale (Fig. 2A). Some linear fractures, generated during thin section preparation, occurred where the stringers were abundant. Several fractures, up to 300 μm in size, were filled with pseudospar calcite and secondary silica (Fig. 2B).

A burrow, 120 μm wide and filled with calcite, was observed. Pyrite and other heavy minerals were present in minor amounts.

The Pumpkin Valley Shale contained two distinct types of laminations. The first type consisted of brown clay and black amorphous organic matter with few detrital grains (Fig. 2C). The second type was translucent and was composed of detrital quartz grains, micas, and glauconite (Fig. 2D). The detrital grain laminations were further subdivided into finer (30- to 50- μm) and coarser (90- to 200- μm) grain sizes. These two subtypes were separated by the organic and clay-rich laminae. The fine-grained lamina was slightly darker in color than the coarse-grained lamina, due either to its fine-grained nature or to the presence of more organic material and iron oxide coatings. Fractures filled with secondary quartz or calcite were common in the shale. Some glauconite peloids (100 to 200 μm) were common in the detrital laminae; many were partially altered and had changed from green color to brown.

Scanning Electron Microscopy

In the Chattanooga Shale, relatively coarse, subangular grains (20 to 50 μm) of quartz and feldspars were observed under backscattered electron beams (Fig. 3A). The feldspars were mostly potassium rich and partially weathered along the edges. Fine (<10- μm) flaky illite was the major component of the shale. The illite was densely compacted, with most of the micropores filled by amorphous organics and occasionally by calcium and barium sulfates. Compressed spore cases, 10 to 30 μm wide and 100 to 200 μm long, were aligned parallel to the general direction of bedding. Some spores were filled with secondary quartz, barite, or pyrite crystals.

Amorphous organics occupied pores of various sizes and shapes (Figs. 3A and B). Cubic and framboidal pyrite was common and often associated with organics and conodonts (Figs. 3C and D).

The Pierre Shale was composed of loosely packed fine grains ($<4 \mu\text{m}$) of smectite and larger-sized grains (10 to $50 \mu\text{m}$) of quartz (Fig. 4A). The sample had a large number of micropores, which might have been generated by partial shrinkage of the smectite due to the loss of sorbed water during sample preparation. Blocky calcite layers ($20 \mu\text{m}$ thick) and fine ($<1 \mu\text{m}$) pseudocubic pyrite grains in between the calcite layers occupied microfractures subparallel to bedding (Fig. 4B). Flaky smectite particles were oriented somewhat randomly (Fig. 4C) and showed fair amounts of calcium and iron in EDX analysis. The presence of calcium and absence of sodium suggested that the exchange sites of the smectite were occupied mainly by calcium. Detrital biotite grains, identified by the presence of K as well as Fe, Mg, Al, and Si, were observed in a fractured sample (Fig. 4D).

The Green River Formation was drastically different from the other shales in terms of morphology and mineralogy. The polished section of the formation showed densely packed aggregates of finely textured ($<2\text{-}\mu\text{m}$) carbonate grains and irregularly shaped and sized pores filled with kerogen. In the carbonate grains, calcium was the dominant cation, but there were considerable amounts of magnesium and occasionally iron and manganese. The matrix appeared to be a mixture of micrite and dolomicrite. A recrystallized iron-carbonate (ankerite) grain, with pyrite concentrated on the surface and in the fractures, was observed (Fig. 5A). Relatively fine grains ($<20 \mu\text{m}$) of quartz and feldspars were distributed throughout

the matrix. SEM examination of a fractured surface demonstrated again the relative uniformity of texture in the formation (Fig. 5B). The grains were aggregated and cemented by calcium carbonate and siliceous material, based on detection of Si with Ca and Mg spectra in EDX analysis. In the close-up micrographs, randomly oriented mineral grains of variable sizes and shapes were observed, along with micropores occupied by organics (Figs. 5C and D).

In the polished sections of the Nolichucky Shale, fine-silt-size detrital quartz, feldspars, dolomite, and calcite were observed in a clay mineral matrix (Figs. 6A and B). Illite was the dominant matrix mineral, but considerable amounts of chlorite and micas were present. In the fractured sample, microfractures and pores were observed between illite packets (Figs. 6C and D). Chlorite was much more prominent. It had a relatively high iron content and was tentatively identified as an iron-rich chlorite.

The Pumpkin Valley Shale was similar in mineralogical composition to the Nolichucky Shale. However, illite grains in the Pumpkin Valley Shale were much more randomly oriented (Fig. 7A). Relatively long packets (10 to 100 μm long and $<10 \mu\text{m}$ thick) of iron-rich chlorite were common in the sample. The SEM examination showed thick chlorite packets with relatively clean surfaces and illites as aggregates with extensive coatings. There were a considerable number of pores that appeared to be filled with organic matter. Calcite was present in detrital form as well as a fracture-filling material (Fig. 7B). Authigenic quartz and framboidal pyrite were common in micropores and microfractures (Figs. 7C and D).

High-Resolution Transmission Electron Microscope Analysis

High-resolution transmission electron microscopy (HRTEM) including energy dispersive X-ray spectrometry of undisturbed shale samples provides crucial information on mineral composition and structure, matrix composition, and micromorphology, which can not be determined by other techniques (Lee et al. 1975a, b; Bell 1986; and Klimentidis and Mackinnon 1986). The observed lattice fringes in the micrographs correspond to the (001) d-spacings of the clay minerals. They were formed by combining the beams diffracted by Rutherford interactions with crystal planes and zero-order transmitted beams. Besides the fringe image measurements, layer silicate minerals were also identified by differences in their chemical composition, as analyzed by qualitative EDX. Besides Si, which was common in all the silicates, illite had moderate amounts of Al and Fe with K, muscovite had Al with K, biotite had high amounts of Fe with K, chlorite had high amounts of Mg and Fe with very low amounts of Al and K, and kaolinite had high amounts of Al and no Mg, Fe, or K.

Clays and detrital grains in the Chattanooga Shale were closely packed, and pores were filled with organic matter (Fig. 8A). Layer silicate minerals were preferentially aligned along bedding planes when they were not interrupted by larger detrital grains. Organic materials were unstable and progressively formed damaged spots under the electron beam. Many thin packets (5 to 20 nm) of illite having 0.5-nm (002) lattice fringes were observed. Occasionally, a thicker (>50-nm) detrital muscovite having 0.5-nm (002) lattice fringes was observed. Chlorite with 1.4-nm fringes was also observed in the sample (Fig. 8B).

Preparation of Pierre Shale specimens by ion milling was very difficult because the sample had very weak cementation between clay particles. In future studies, a low-viscosity bonding agent will be introduced prior to ion milling. HRTEM analysis of the sample indicated that smectite aggregates were randomly oriented, showing both (hk0) and (001) planes in the same area (Fig. 9A). Some of the clays showed 1.2-nm lattice fringes, but 1.0-nm fringes were more common in the sample (Fig. 9B). The clays were composed mainly of Si, Al, and Ca, with trace amounts of Fe and K, which indicated that they were predominantly dioctahedral calcium-montmorillonite. There was no evidence of interstratified illite/smectite mineral in the sample. Since the montmorillonite can be thermally altered, further detailed study is warranted for understanding waste-induced thermal effects on swelling clays.

The Green River Formation was hard and mechanically stable during specimen preparation. It had no preferred fracture orientation, as did the other samples. The minerals were apparently cemented by amorphous silica (Fig. 10A). The characteristics of the cemented phase should be reexamined by other methods because it is important for understanding the chemical stability of the formation. The dominant minerals were rhombohedral dolomite, quartz, calcite, and micas. A higher magnification of the mica particles showed well-defined 1.0-nm fringes (Fig. 10B). The chemical composition of the mica was close to muscovite, but it contained a small amount of iron. A thin particle with morphological features close to illite was observed next to the large mica particle shown in Figure 10B.

The Nolichucky Shale had many thin (10- to 100-nm) packets of illite that parallel or cross one another (Fig. 11A). The large spaces (1.2 to 1.4 nm) occurring between the packets could be a chlorite fringe, but such spaces could result from other causes. Thin illite packets (1.0-nm lattice fringes) occurred between thick (>100-nm) mica particles, which also had well-defined 1.0-nm lattice fringes (Fig. 11B). Illite was differentiated from mica only by morphological features, since both phases show similar chemical compositions in EDX analysis. Disappearance of fringes between illite packets was caused by the misalignment of the illite packet toward the electron beam in those areas. Carbonate cementation was observed but was not common in this specimen.

The Pumpkin Valley Shale was also a difficult sample for HRTEM analysis because of the lack of cementation between minerals and the presence of abundant micropores between randomly oriented illite packets (Fig. 12A). There were few areas in which illite particles were properly oriented toward the electron beam. These illites, like those in the Nolichucky Shale, had thin packets of 1.0-nm lattice fringes (Fig. 12B).

The noticeable differences in microstructure of the shales cause large differences in their BET surface areas. The surface area of the samples ranged from 23.79 to $1.92 \text{ m}^2 \cdot \text{g}^{-1}$, with the following order: Pierre > Nolichucky > Pumpkin Valley > Chattanooga > Green River (Table 1). The lower surface areas of the Chattanooga and Green River samples resulted from the extensive cementation observed between primary particles, which prevented penetration of nitrogen gas to the primary particle surfaces, thus reducing the measured surface areas.

The surface area measurements suggest that radionuclides and leaching solutions would have greater access to the surfaces of primary particles of the Pierre, Nolichucky, and Pumpkin Valley shales and lesser access to the surfaces of primary particles of the Chattanooga and Green River shales. Therefore, the diffusion rates through the shales and the kinetics of sorption of radionuclides onto the shales should be carefully evaluated. If some equilibrated radionuclides diffuse into the aggregates during sorption experiments, reversibility should be also determined under the same conditions. Sorption kinetics can be determined through standard sorption experiments, but microscopic analysis of radionuclide-equilibrated block samples would be more useful and realistic.

Semiquantitative Mineral Composition

Semiquantitative estimation of the mineralogical composition of shales is a very difficult task, but it is necessary for many reasons. In nuclear waste disposal studies, data on mineralogical composition would be helpful for predicting groundwater composition, interpreting sorption and desorption results and physical properties, and providing the data base for modeling radionuclide transport. There are many different approaches to quantitative mineralogical analysis (e.g., Schultz 1964; Jackson 1975), but there is no standard method established by the clay mineral research community. The major problem encountered, when an attempt is made to establish a standard method, is the extreme variability among sedimentary rocks in mineral composition, in mineral crystallinity, and in the effects of diagenesis and weathering on clay minerals, as illustrated by the shales selected for this investigation. Therefore, a combination of specifically

applicable analytical techniques for the semiquantitative estimation of the mineral composition of the five shale samples was used in this study.

The results presented in Table 1 are semiquantitative in nature, and careful refinement of each analytical method, with cross-checking by independent methods, is needed. Organic matter and water contents of the shales were estimated from thermal analyses. Carbonate contents were calculated from CO_2 evolution data obtained through acid dissolution and thermal analysis. Pyrite contents were calculated from the sulfide contents. The chemical compositions of whole-rock samples of the shales analyzed by wet chemical methods and neutron activation are summarized in Table 2. Quartz plus feldspar contents were determined by SEM backscattered electron image analysis of thin section slides. Feldspars, a minor component in these samples, were included in the quartz contents. Phyllosilicates were estimated from chemical analysis data (potassium content), XRD peak area ratio, and both backscattered electron image and X-ray dot-mapping analyses. The estimates were recalculated with the particle-size distribution results (Lee et al. 1987).

Semiquantitative mineralogical analyses showed that the Chattanooga Shale was composed of 49% illite, 25% quartz plus feldspar, 11% organic matter, 6% pyrite, and 4% chlorite plus kaolinite. Microcline-orthoclase was dominant among the feldspars, and both chlorite and kaolinite were present in the sample. The Chattanooga Shale was an illite-rich shale but one that also was relatively rich in organic matter and pyrite in comparison with other illitic shales. Both constituents would play an important role in its geochemical behavior.

The Pierre Shale contained 59% smectite, which appeared to be calcium-saturated montmorillonite. Other minerals occurring in the shale were 15% carbonates, 11% quartz plus feldspars, 5% organic mineral among the carbonates, and feldspars were insignificant in the sample. The Pierre Shale is expected to have a high cation exchange capacity and swelling potential compared with the other shales.

The Green River Formation was selected as a carbonate end-member shale, but it also contained a considerable amount of organic matter. The shale was composed of 42% carbonates, 28% quartz plus feldspars, 13% organic matter, and 10% illite. Dolomite appeared to be the dominant carbonate, but a considerable amount of calcite was present. The organic matter, in the form of kerogen, coated the mineral components and filled the micropores. The hydrophobic nature of organic-coated minerals would hinder their interaction with aqueous solutions. Therefore, the Green River Formation is not a typical carbonate-rich shale, and the program may need to identify another carbonate shale that is relatively free of kerogen for evaluation. The difference in the degree of maturity of the organic matter in the Green River Formation and that in the Chattanooga Shale, makes for a useful comparison of alternative organic-bearing shales.

The Nolichucky Shale is an illitic shale containing carbonate but without organic matter. The sample was composed of 43% illite, 29% quartz plus feldspars, 14% chlorite plus kaolinite, and 11% carbonates. The carbonate in the sample was mostly fracture-filling secondary calcite. Iron-rich chlorite was the dominant phase in the chlorite plus kaolinite component. The feldspar phase was not fully analyzed. Since carbonate is

the most soluble component in the sample, its possible effects on the geochemical behavior of this illitic shale should be determined.

The Pumpkin Valley Shale was composed of 57% illite, 22% quartz plus feldspars, and 15% chlorite plus kaolinite. Analyses indicated the occurrence of both chlorite and kaolinite, but a separate estimation of each individual mineral was not attempted. The chlorite in the shale behaved as iron-rich chamosite. Further analysis of feldspars is also needed. Nevertheless, the Pumpkin Valley Shale appears to be an excellent example of an illitic end-member shale, which is relatively low in organic matter, carbonates, and pyrite.

The semiquantitative mineralogical analyses indicated that the shales selected as end-members of carbonaceous, illitic, smectitic, and carbonate shales appear to fulfill programmatic objectives. They are not true end-members by any means, but they are probably better than standard mineral samples for our purposes. If there are compositional parameters that should be of high priority in the ultimate selection of a particular type of shale for a repository site, information gained from this study could be invaluable in helping to selectively narrow down the number of potential shale units for further study during a national survey.

SUMMARY

Shale is a complex rock and can have many different mineral, organic, and elemental components. Each component has a different role in radionuclide retardation and groundwater-shale interaction, and each has different thermal, mechanical, and hydrologic properties.

Four end-member shales were selected on the basis of their composition for comprehensive microstructural and mineralogical characterization: the Chattanooga Shale was selected as representing a carbonaceous shale, the Pierre Shale as a smectitic shale, the Green River Formation as a carbonate-rich shale, and the Nolichucky Shale and Pumpkin Valley Shale as illitic shales.

The Chattanooga Shale had a relatively low surface area ($4.6 \text{ m}^2 \cdot \text{g}^{-1}$) considering its moderately high clay content (35%), suggesting extensive compaction and cementation of the particles. It was composed of 49% illite, 25% quartz plus feldspar, 11% organic matter, 6% pyrite, 4% chlorite plus kaolinite, and other accessory minerals. Microscopic analyses indicated that the mineral components of the shale were highly compacted, and micropores were filled with organic matter. Carbonate and sulfate cements were present but were not common. The organic matter was apparently unstable under a prolonged low-temperature heat treatment (250°C for 6 months), as indicated by the disappearance of an exothermic peak representing organics in the differential thermal analysis after the heat treatment. The high organic and pyrite contents but near absence of carbonate in this shale are significant characteristics because they may at

least partially control solution chemistry when they are equilibrated with radionuclide-containing groundwater.

The loosely packed Pierre Shale had a high surface area ($23 \text{ m}^2 \cdot \text{g}^{-1}$) as well as a high clay content (69%). It contained 59% smectite, 15% carbonate, 11% quartz plus feldspar, 5% organic matter, 3% mica, and 2% pyrite. Micropores and fractures were frequently observed in the sample. Carbonate minerals had grown in the fractures but did not cement the clay minerals. Calcite was the principal carbonate in the sample. The smectite, identified as montmorillonite, has a high cation exchange capacity. The cation exchange sites in the sample were saturated with calcium that could be replaced by radioactive cations released from waste packages. Montmorillonite also has a very high swelling capacity, an important engineering characteristic for seal and backfill materials. The micropores and fractures observed in a dehydrated state of this shale would be sealed by the swelling of montmorillonite clays when they are rehydrated by groundwater.

The shale sample from the Green River Formation was hard and structurally stable and had a very low surface area ($2 \text{ m}^2 \cdot \text{g}^{-1}$) for the rather large amount of clay-sized particles (46%). It was composed of 42% carbonates, 28% quartz plus feldspar, 13% organic matter, and 10% illite. The Green River Formation was selected primarily as a carbonate end-member shale, but the analyses indicated that it also contained a considerable amount of organic matter. The organic matter appeared to be a liquid hydrocarbon, rather than the solid matter found in the Chattanooga Shale. Hydrocarbon had coated the mineral components and filled the micropores in the shale, which hindered interaction of the

minerals with aqueous solutions because of the hydrophobic nature of the coating. Dolomite was the dominant carbonate, but a considerable amount of calcite was present. Dolomite and other crystalline mineral components were cemented by amorphous silica and carbonates. Such extensive cementation gave physical stability to the shale and locked the organic matter in isolated micropores.

The Nolichucky Shale had a moderate surface area ($15 \text{ m}^2 \cdot \text{g}^{-1}$) for its clay content (51%). It was composed of 43% illite, 29% quartz plus feldspar, 14% chlorite plus kaolinite, and 11% carbonates, which is typical for illitic shales with carbonates and without organic matter. Thin illite packets with 1-nm lattice fringes, which were observed under high-resolution transmission electron microscopy, could provide sorption sites for radionuclides. Iron-rich chlorite was the dominant phase in the chlorite plus kaolinite component. A major portion of the carbonate was fracture-filling secondary calcite, but detrital dolomite and calcite were also observed.

The Pumpkin Valley Shale, a laminated mudstone and siltstone, had a moderate surface area ($13 \text{ m}^2 \cdot \text{g}^{-1}$) and moderate clay content (30%) and contained 57% illite, 22% quartz plus feldspar, and 15% chlorite plus kaolinite. This was a more representative illitic shale, since it had only trace amounts of carbonates, organic matter, and pyrite. Clay particles in the shale were loosely packed and randomly oriented. Cementation was rarely observed in the mudstone but was common in the siltstone laminae. The presence of micropores was frequently observed among phyllosilicate packets. Both chlorite and kaolinite were present in the sample.

This investigation revealed that the shales selected as end-members of carbonaceous, smectitic, carbonate, and illitic shales have a wide range of microstructural and mineralogic characteristics that would be related to the performance of shale as a nuclear waste repository. Distribution of micropores and fractures, degree of cementation, mineral orientation, and mineralogical composition are a few of the features that could control the mobility of radionuclides released from wastes and geochemical conditions related to the stability of waste package materials. The results of the microstructural and mineralogical analyses are critical data for the interpretations of thermal properties, hydrologic behavior, and sorption properties of shale formations.

REFERENCES

Bell, T. E., 1986. Microstructure in mixed-layer illite/smectite and its relationship to the reaction of smectite to illite. *Clays and Clay Minerals*, v. 34, p. 146-154.

Burkett, P. J., R. H. Bennett, H. Li, F. L. Nastav, W. R. Bryant, L. E. Shephard, and W.-A. Chiou, 1987. Microstructure of red clay from the central Pacific Deep-Sea Basin: Significance to subseabed nuclear waste disposal. SAND86-2492, Sandia National Laboratories, Albuquerque, New Mexico.

Conant, L. C., and V. E. Swanson, 1961. Chattanooga Shale and related rocks of central Tennessee and nearby areas. U.S. Geol. Surv. Prof. Paper 357. U.S. Government Printing Office, Washington, D.C.

Croff, A. G., T. F. Lomenick, R. S. Lowrie, and S. H. Stow, 1986. Evaluation of five sedimentary rocks other than salt for geologic repository siting. ORNL-6241, Oak Ridge National Laboratory, Oak Ridge, Tennessee.

Gera, F., 1980. Summary of replies to the questionnaire on R&D activities relevant to the disposal of radioactive wastes in argillaceous formation. Proc., Workshop on the Use of Argillaceous Materials for Isolation of Radioactive Waste, NEA/OECD, Paris, 1979. p. 11-13.

Güven, N., C. R. Landis, and G. K. Jacobs, 1988. Characterization of clay minerals and organic matter in shales: Application to high-level nuclear waste isolation. ORNL/TM-10759, Oak Ridge National Laboratory, Oak Ridge, Tennessee.

Jackson, M. L., 1975. Soil Chemical Analysis--Advanced Course. 2nd ed.

Department of Soil Science, University of Wisconsin, Madison.

Klimentidis, R. E., and I. D. R. Mackinnon, 1986. High-resolution imaging of ordered mixed-layer clays. *Clays and Clay Minerals*, v. 34, p. 155-164.

Lee, S. Y., L. K. Hyder, and P. D. Alley, 1987. Mineralogical characterization of selected shales in support of nuclear waste repository studies. ORNL/TM-10567, Oak Ridge National Laboratory, Oak Ridge, Tennessee.

Lee, S. Y., M. L. Jackson, and J. L. Brown, 1975a. Micaceous vermiculite occlusions in kaolinite observed by ultramicrotomy and high resolution electron microscopy. *Clays and Clay Minerals*, v. 23, p. 125-129.

Lee, S. Y., M. L. Jackson, and J. L. Brown, 1975b. Micaceous vermiculite, glauconite, and mixed-layered kaolinite-montmorillonite examination by ultramicrotomy and high resolution electron microscopy. *Soil Science Society of America Journal*, v. 39, p. 793-800.

Lee, S. Y. and R. W. Tank, 1985. Role of clays in the disposal of nuclear waste: A review. *Applied Clay Science*, v. 1, p. 145-162.

Lomenick, T. F., and R. B. Laughon, 1980. A regional characterization of the Devonian Shales in the Eastern U.S. for the storage/disposal of radioactive wastes. Proc., Workshop on the Use of Argillaceous Materials for the Isolation of Radioactive Waste, NEA/OECD, Paris, 1979: p. 121-128.

Milodowski, A. E., A. J. Bloodworth, and R. D. Wilmot, 1985. Long term effects on potential repository sites: The alteration of the Lower Oxford Clay during weathering. FLPU 85-13, British Geological Survey, London.

Schultz, L. G., 1964. Quantitative interpretation of mineralogical composition from X-ray and chemical data for the Pierre Shale. Geol. Surv. Prof. Paper 391-C, U.S. Government Printing Office, Washington, D.C.

Stow, S. H., and A. G. Croff, 1987. The potential for use of clay-rich strata as a host medium for a high-level nuclear waste repository. Abstract. 24th Clay Mineral Society Meeting, Socorro, New Mexico, October 20, 1987. p. 124.

Von Damm, K. L., 1987. Geochemistry of shale groundwaters: Survey of available data and postulated mineralogic controls on composition. ORNL/TM-10488, Oak Ridge National Laboratory, Oak Ridge, Tennessee.

Weaver, C. E., 1979. Geothermal alteration of clay minerals and shales: Diagenesis. ONWI-21, Office of Nuclear Waste Isolation, Battelle Memorial Institute, Columbus, Ohio.

FIGURE LEGENDS

Fig. 1. Photomicrographs of shales in transmitted light.

(A) Chattanooga Shale with framboidal pyrite, p. (B) Pierre Shale with ostracods (arrows). (C) and (D) Green River Formation, showing heavy mineral concentration (arrow).

Fig. 2. Photomicrographs of shales in transmitted light.

(A) Nolichucky Shale with stair-step fracture. (B) Nolichucky Shale with calcite vein filling. (C) Pumpkin Valley Shale, showing organic matter, o, and coarse detrital grains. (D) Pumpkin Valley Shale, showing fine detrital grains and glauconite, g.

Fig. 3. Scanning electron micrographs of Chattanooga Shale.

(A) Backscattered electron image of polished section, showing quartz, q; feldspar, f; chlorite, ch; pyrite, p; organics, o; and spores, s. (B) Secondary electron image of fractured rock, showing spores, s; barite, b; quartz, q; and pyrite, p. (C) Secondary electron image, showing bedding. (D) Pyrite, p, surrounded by illite, i.

Fig. 4. Scanning electron micrographs of Pierre Shale. (A) Smectite, s; feldspar, f; and quartz, q, grains. (B) Calcite, c, and pyrite, p, in microfractures subparallel to bedding. (C) Illite, i, in smectite, s, matrix. (D) Detrital biotite, b, associated with a fracture, plus pyrite, p, and smectite, s, grains.

Fig. 5. Scanning electron micrographs of Green River Formation.

(A) Polished section, showing pyrite, p; calcite, c; and quartz, q, in dolomicrite matrix. (B) Fractured surface, showing quartz, q, and feldspar, f, in dolomicrite. (C) Enlargement of B, showing feldspar, f, and micropore, po. (D) Possible aragonite, a, in dolomicrite matrix.

Fig. 6. Scanning electron micrographs of Nolichucky Shale.

(A) Polished section, showing detrital quartz, q; calcite, c; feldspar, f; and chlorite, ch. (B) Polished section, showing detrital calcite, c; chlorite, ch; quartz, q; dolomite, d; and a titanium mineral, t. (C) Fractured surface, showing clinochlorite grain, cl, and pores, po, in illite matrix. (D) Fractured surface, showing quartz, q, and feldspar, f.

Fig. 7. Scanning electron micrographs of Pumpkin Valley Shale.

(A) Polished section, showing quartz, q; chlorite, ch; and a microfracture (arrow) in a matrix of randomly oriented illite. (B) Fracture-filling calcite, c, and quartz, q, with detrital calcite grain (arrow) in an illite matrix. (C) Authigenic quartz, q; chlorite, ch; and illite, i, in a micropore. (D) Framboidal pyrite, p.

Fig. 8. High-resolution transmission electron micrographs of Chattanooga Shale. (A) Illite packets, i, with organic matter, o, and pyrite, p. (B) Illite packets, i, between mica, m, and chlorite, ch.

Fig. 9. High-resolution transmission electron micrographs of Pierre Shale. (A) Random orientation of smectite aggregates, s. (B) 1.2-nm lattice fringes of smectite.

Fig. 10. High-resolution transmission electron micrographs of Green River Formation. (A) Dolomite, d; quartz, q; and mica, m, grains and siliceous cement, Si. (B) 1-nm fringes on mica grain, m, and illite grain, i.

Fig. 11. High-resolution transmission electron micrographs of Nolichucky Shale. (A) Illite packets, i, with discontinuities (arrow). (B) Illite packets, i, between mica particles, m.

Fig. 12. High-resolution transmission electron micrographs of Pumpkin Valley Shale. (A) Micropores, po; quartz, q; and random orientation of illite packets, i. (B) 1-nm lattice fringes.

Table 1. Chemical composition, surface area, and particle-size distribution of whole-rock samples

	Chattanooga Shale	Pierre Shale	Green River	Nolichucky Shale	Pumpkin Valley
Chemical composition (weight percent)					
SiO ₂	57.78	49.22	34.24	40.66	62.06
Al ₂ O ₃	13.61	13.99	7.56	13.04	20.79
K ₂ O	3.95	2.27	3.25	3.41	5.37
Na ₂ O	0.38	0.66	0.70	0.34	0.66
FeO	5.79	5.40	2.70	3.99	6.69
TiO ₂	0.77	0.48	0.27	0.48	0.80
MgO	1.35	2.17	6.35	2.34	2.00
CaO	0.27	8.58	13.16	6.02	0.29
CO ₃	<0.50	10.50	26.40	9.60	<0.50
SO ₄	0.32	0.26	0.12	0.18	0.10
Sulfide	4.22	0.89	0.30	0.12	0.26
Particle-size distribution (weight percent)					
180-53 μm	1	1	1	1	7
53-2 μm	64	31	54	49	63
2-0.2 μm	26	19	14	21	18
<0.2 μm	9	50	32	30	12
Surface area ($\text{m}^2 \cdot \text{g}^{-1}$)					
Surface area	4.6	22.8	2.0	15.2	12.6

Table 2. Estimated mineralogical composition of whole-rock samples of shale^a

	Chattanooga Shale	Pierre Shale	Green River	Nolichucky Shale	Pumpkin Valley
(weight percent)					
Organic matter	11	5	13	t	t
Chlorite + kaolinite	4	t	t	14	15
Illite	49	t	10	43	57
Micas	t	4	t	t	t
Smectite	nd	59	nd	nd	nd
Carbonates	t	15	42	11	t
Quartz-feldspars	25	11	28	29	22
Pyrite	6	2	t	t	t
Weight loss (105°C)	1	4	2	2	2

^at = trace (<2%), observed from thin section and electron micrographs.

nd = not detectable.

Fig. 1

ORNL-DWG 07-15047



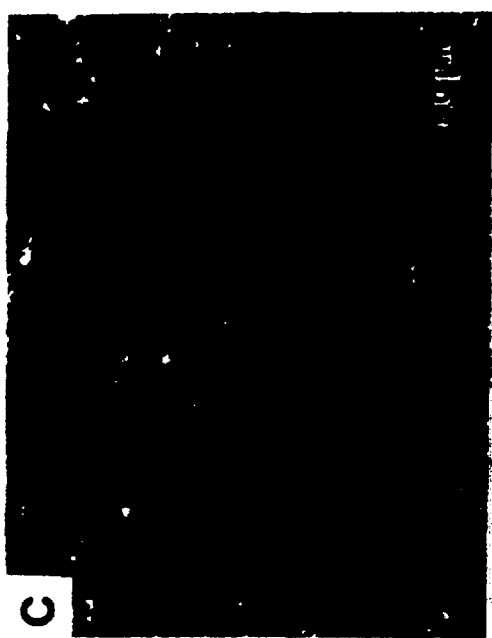
B



D



A



C

REPRODUCED FROM BEST
AVAILABLE COPY

fig. 2

ORNL-DWG 87-15048



A



B



C

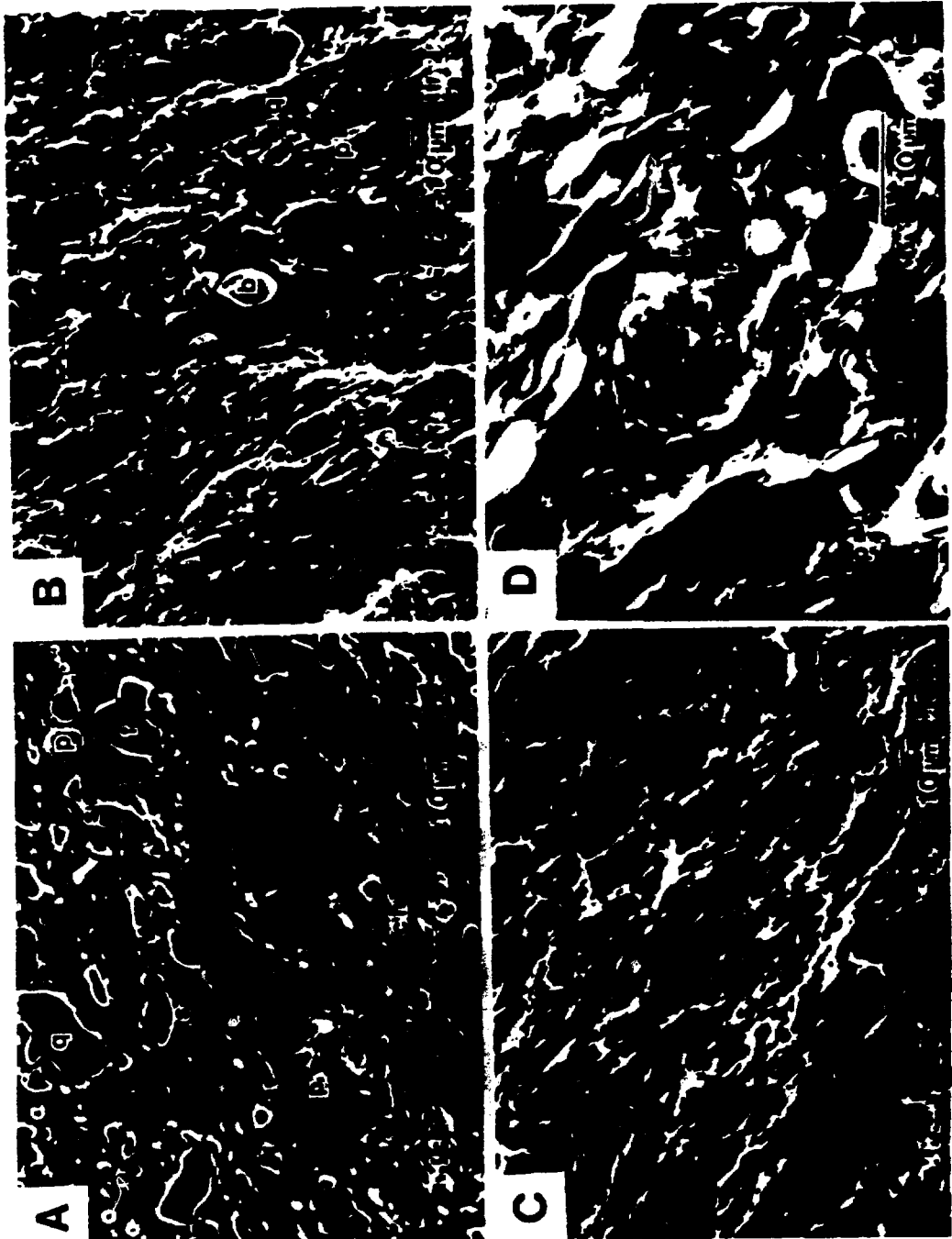


D

REPRODUCED FROM BEST
AVAILABLE COPY

Fig. 3

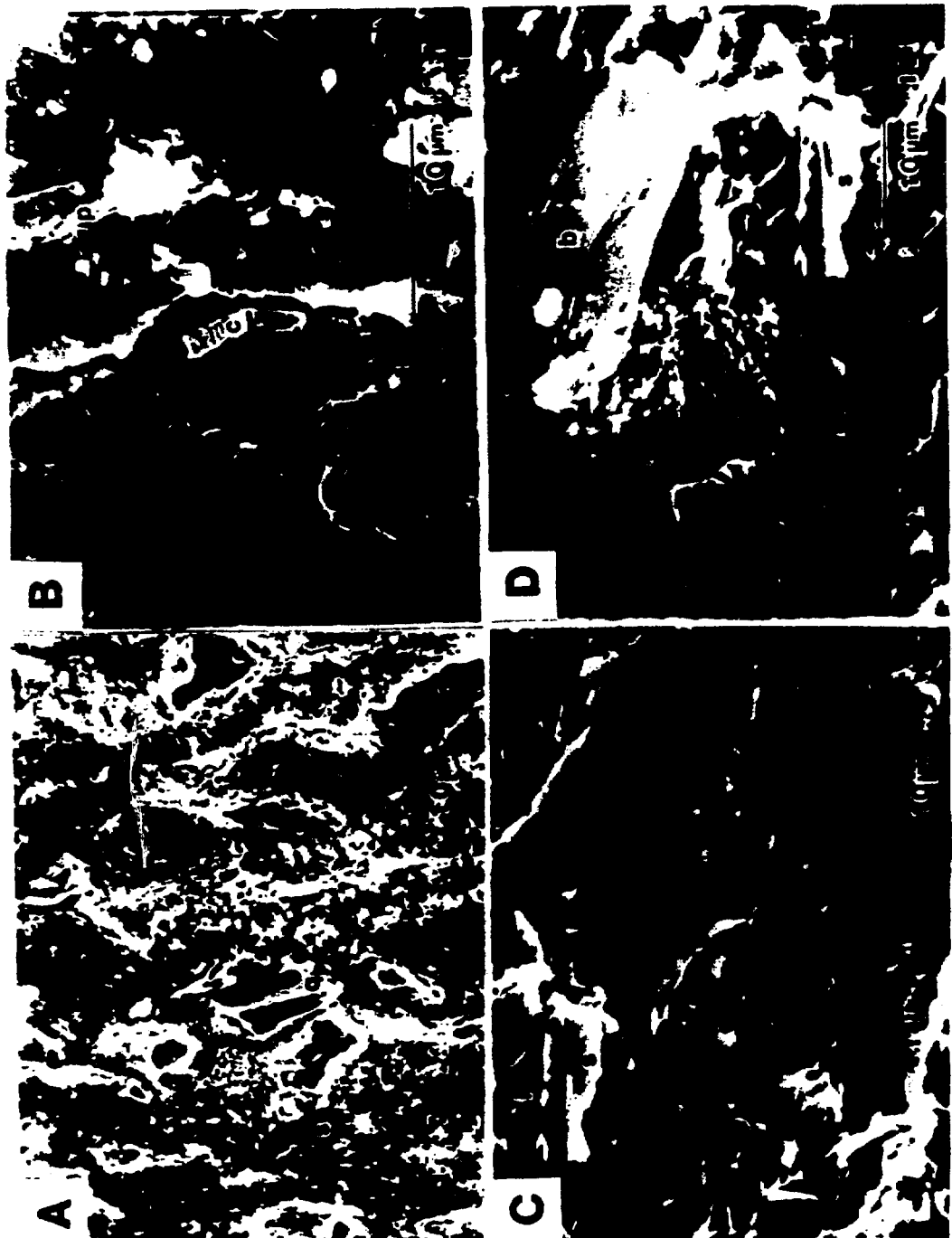
ORNL-DWG 87-15049



REPRODUCED FROM BES
AVAILABLE COPY

Fig. 4

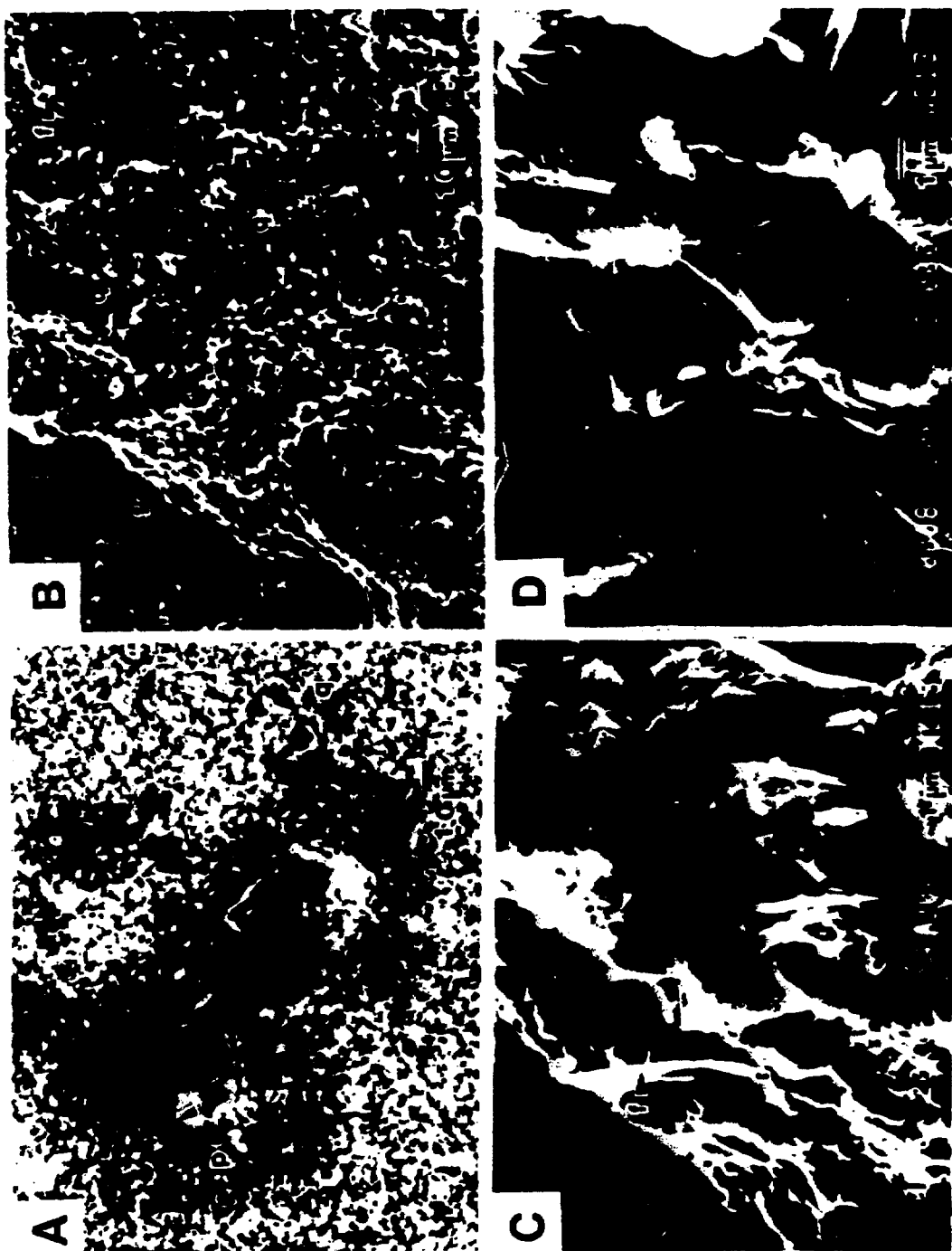
ORNL-DWG 87-15050



REPRODUCED FROM BEST
AVAILABLE COPY

Fig. 5

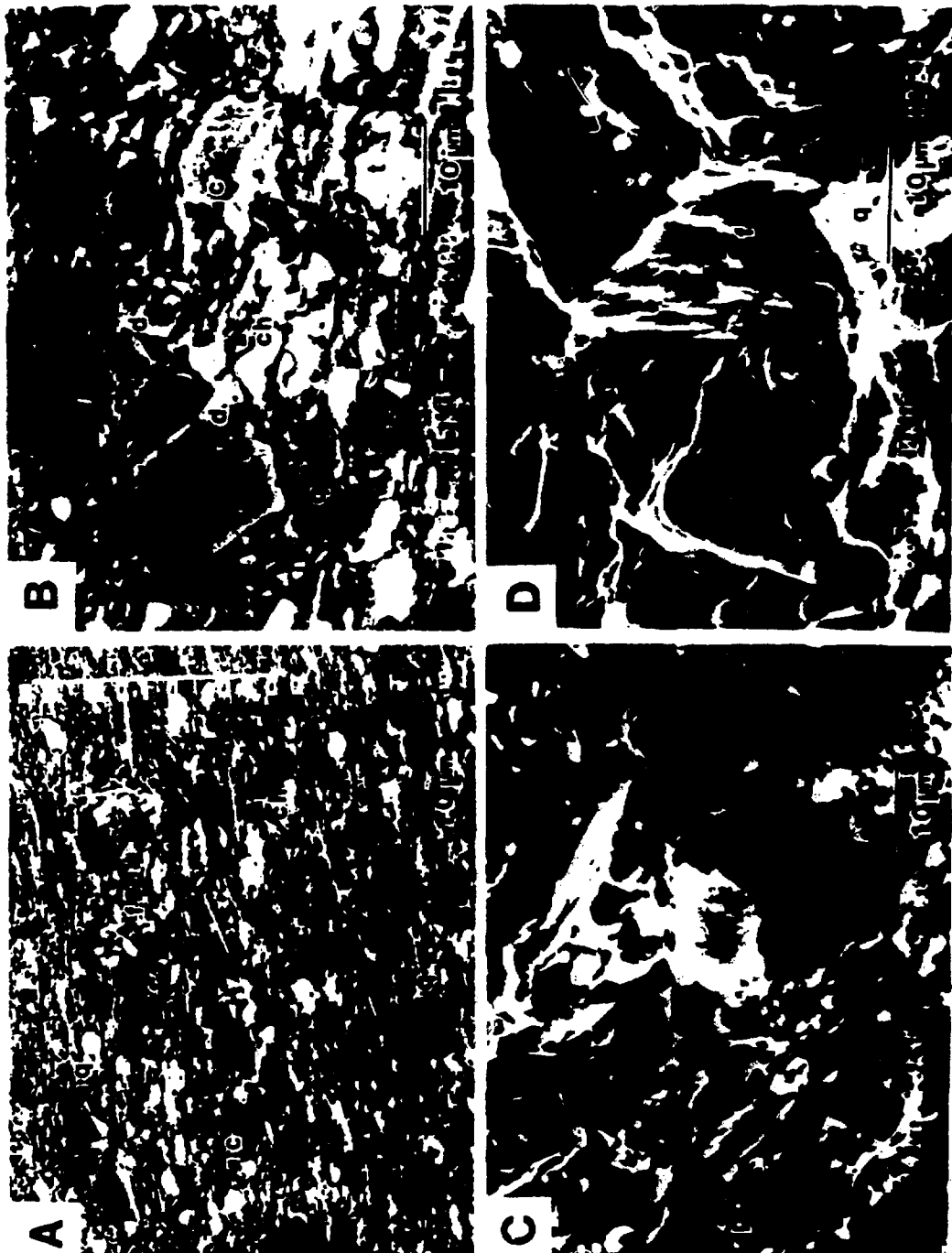
ORNL-DWG 87-15051



REPRODUCED FROM BEST
AVAILABLE COPY

Fig. 6

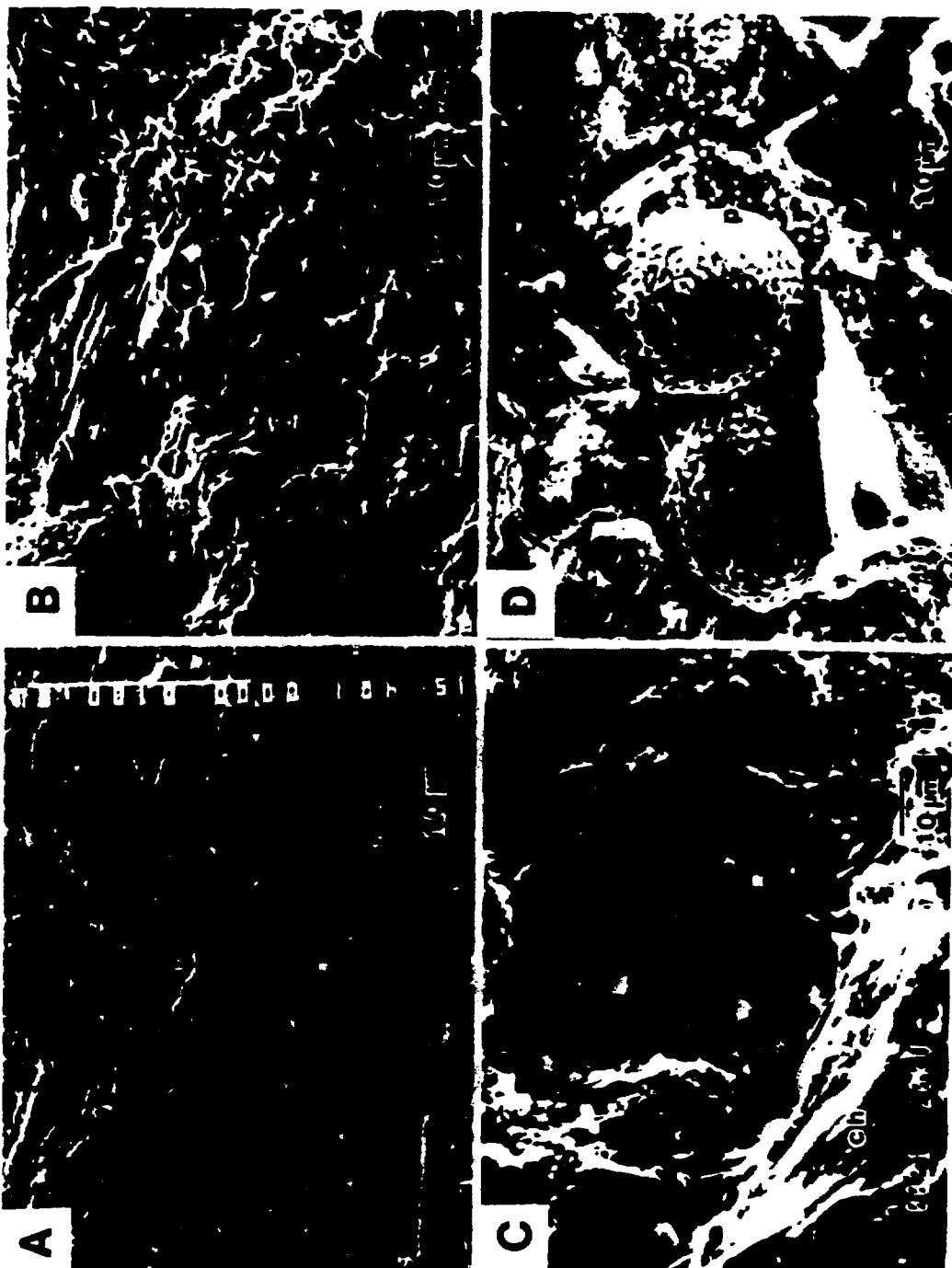
ORNL-DWG 87-15052



REPRODUCED FROM BES
AVAILABLE COPY

Fig. 7

ORNL-DWG 87-15053



REPRODUCED FROM BEST
AVAILABLE COPY

Fig. 8

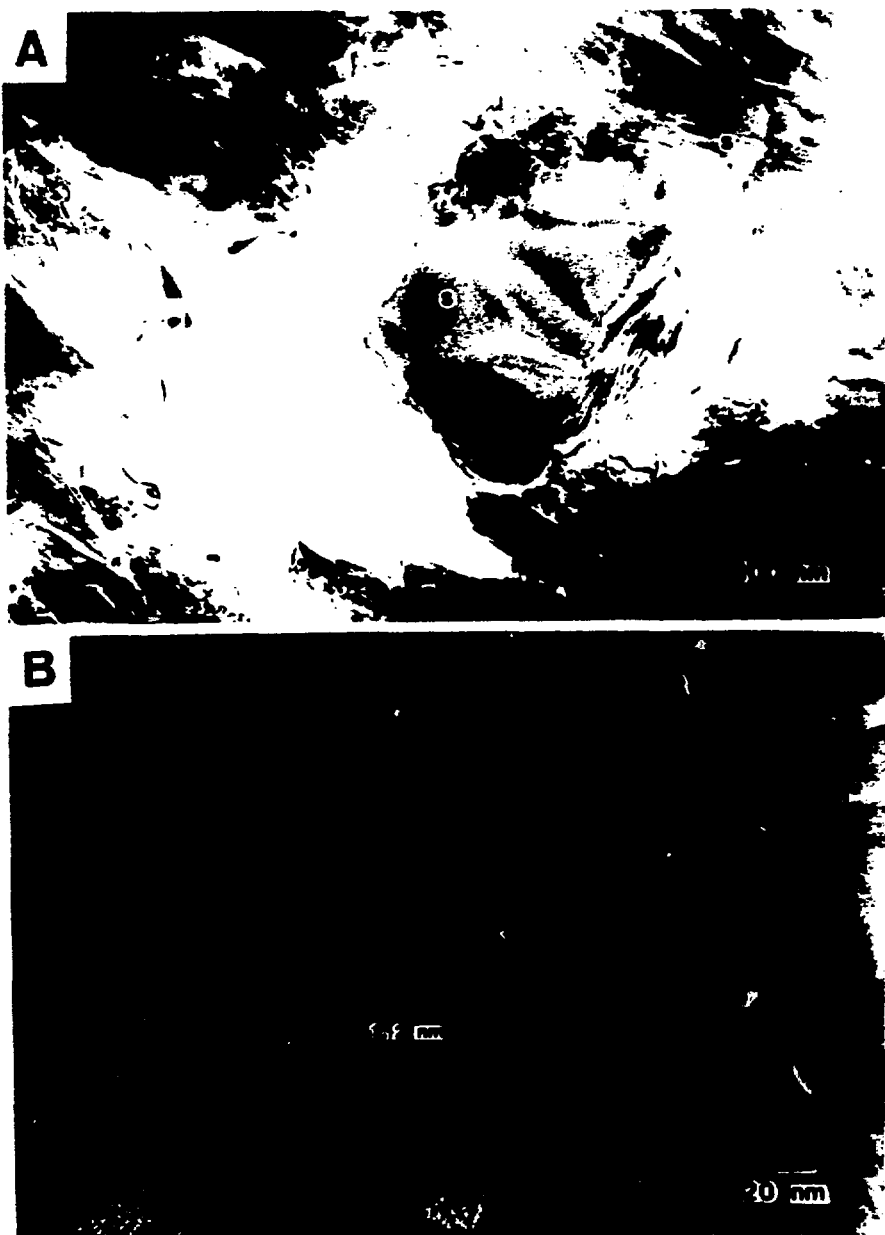
ORNL-DWG 87-15054



REPRODUCED FROM BEST
AVAILABLE COPY

Fig. 9

ORNL-DWG 87-15055

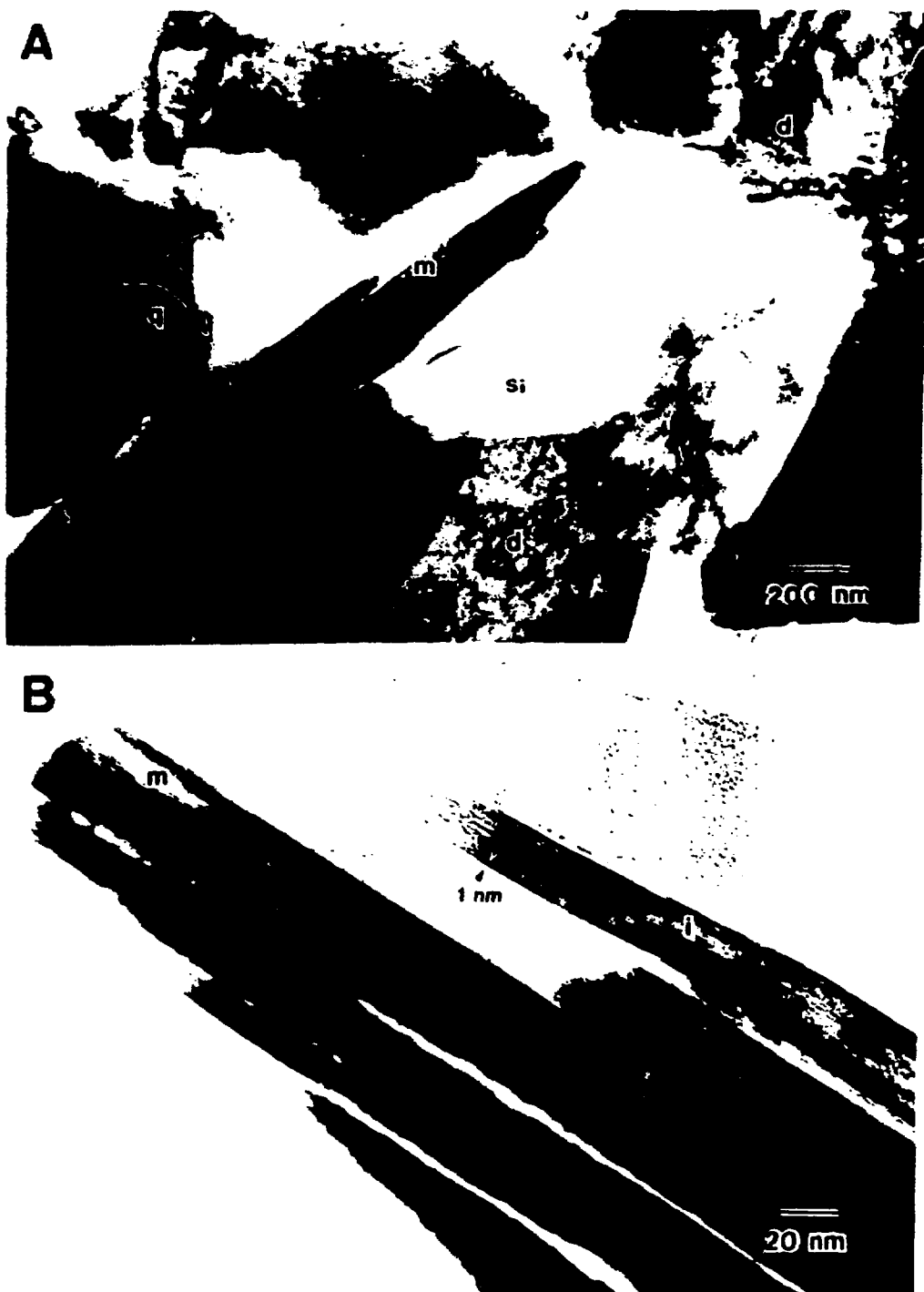


REPRODUCED FROM
AVAILABLE COPY

REPRODUCED FROM BEST
AVAILABLE COPY

Fig. 10

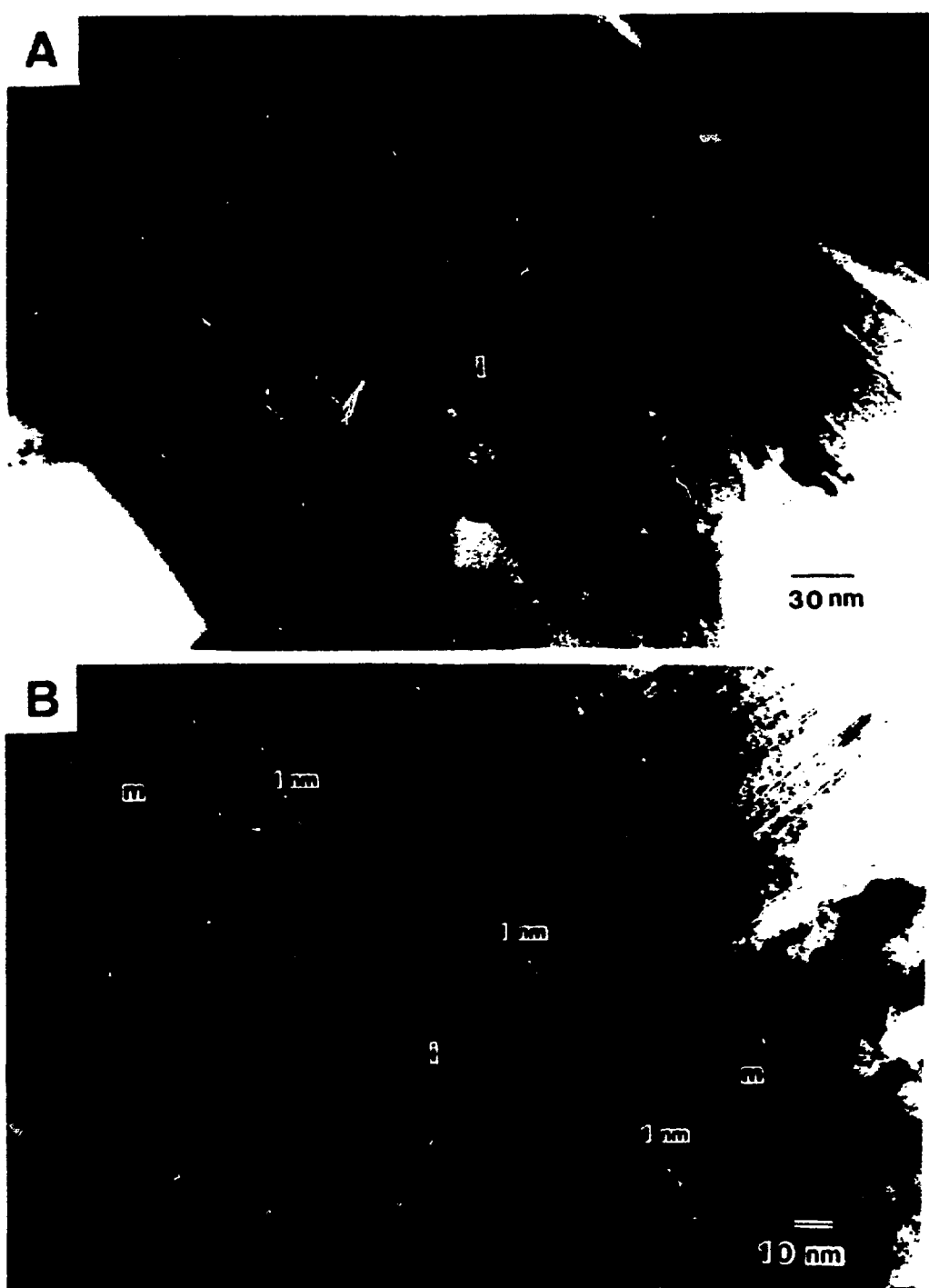
ORNL-DWG 87-15056



REPRODUCED FROM BEST
AVAILABLE COPY

Fig. 11

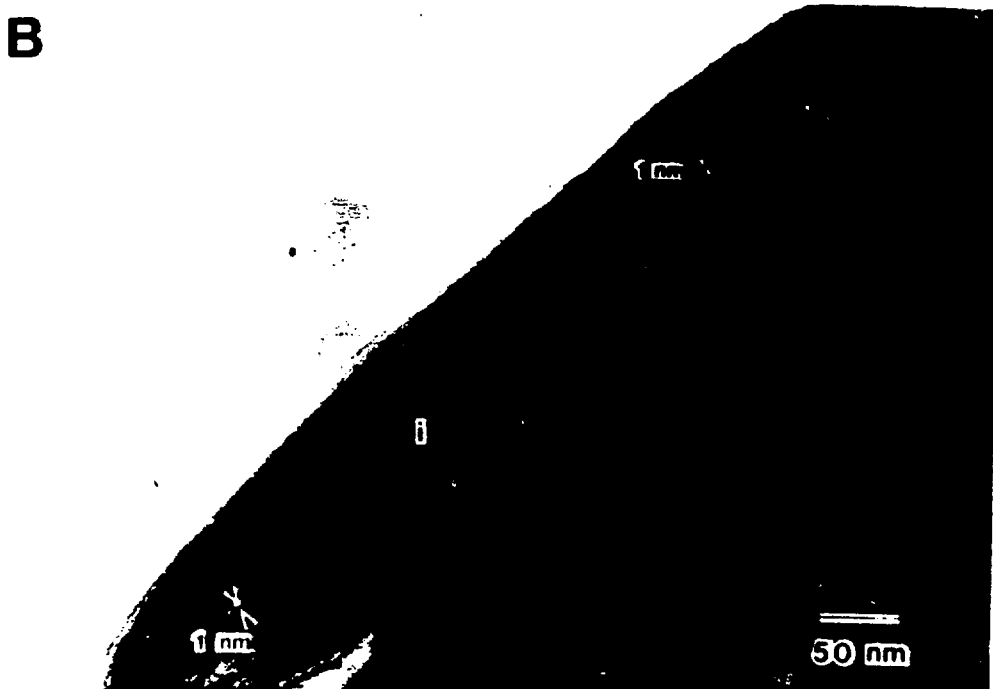
ORNL-DWG 87-15057



REPRODUCED FROM BEST
AVAILABLE COPY

Fig. 12

ORNL-DWG 87-15058



REPRODUCED FROM BEST
AVAILABLE COPY